

Pushing paleoclimate research forward: Direct determination of triple oxygen and carbon isotope ratios of CO₂ by HR-IRMS analysis of fragment ions

Authors: Jakub Surma¹, Getachew A. Adnew², Nina Albrecht³, Issaku E. Kohl³

¹University of Göttingen, Geoscience Center, Göttingen, GER

²University of Utrecht, Institute of Marine and Atmospheric Research, Utrecht, NED

³Thermo Fisher Scientific (Bremen) GmbH, Bremen, GER

Keywords: Stable isotopes, triple oxygen isotopes, $\Delta^{17}\text{O}$, carbon isotopes, clumped carbonate, Δ_{47} , fragment method, paleoclimate, atmosphere, carbon dioxide, HR-IRMS

Goal

This application note describes the capabilities of the Thermo Scientific™ Ultra™ high resolution isotope ratio mass spectrometer (HR-IRMS) to determine the triple oxygen ($\delta^{18}\text{O}$ and $\delta^{17}\text{O}$) and carbon isotope ($\delta^{13}\text{C}$) compositions of CO₂ at high precision by interference-free measurements of oxygen and carbon fragment ions (C⁺ and O⁺). We highlight the advantages of this approach compared to previous methods and outline innovative applications



in paleoclimate research. We particularly emphasize its potential to improve the reliability of clumped carbonate analysis and the possibility to utilize triple oxygen isotopes as an independent geothermometer.

Introduction

Classical oxygen and carbon stable isotopes ($\delta^{18}\text{O}$ and $\delta^{13}\text{C}$) of CO₂ are powerful and established tools to tackle various questions in climate research, paleoclimate reconstruction, atmospheric studies, and palaeoceanography. These isotopic signatures — recorded in atmospheric, geological, or biochemical samples — are controlled by mass-dependent, kinetic and equilibrium fractionation effects. They are utilized to constrain atmospheric gas fluxes, their sources and sinks, and to reconstruct climate histories and environmental conditions.

Besides the classical $\delta^{18}\text{O}$, the analytically challenging measurement of $\delta^{17}\text{O}$ in CO_2 has become a valuable tool to address the above-mentioned questions in a further dimension. The $\Delta^{17}\text{O}$ is defined as a measure of the deviation from the mass-dependent fractionation line in a triple oxygen isotope plot:

$$\Delta^{17}\text{O} = \ln(\delta^{17}\text{O} + 1) - \lambda \cdot \ln(\delta^{18}\text{O} + 1)$$

The factor λ can range from 0.50 to about 0.53 for mass-dependent processes (e.g. Thiemens, 1999; Miller, 2002). The $\Delta^{17}\text{O}$ records mass-independent fractionation processes such as ozone photolysis in the troposphere (e.g. Thiemens et al., 1995; Hoag et al., 2005; Wiegel et al., 2013; Thiemens et al., 2014; Koren et al., 2019), and refines our understanding of kinetic isotope exchange processes between biosphere, geosphere, hydrosphere and atmosphere of the Earth (e.g. Liang et al., 2007; Passey et al., 2014; Hofmann et al., 2017; Adnew et al., 2020) and even extra-terrestrial environments (Farquhar et al., 1998). The combined $\Delta^{17}\text{O}$ and $\delta^{18}\text{O}$ of carbonate CO_2 furthermore have the potential to be utilized as a carbonate single phase paleothermometer (Surma et al., 2019; Jäger et al., 2020).

Because the ^{17}O -bearing bulk isotopologues of CO_2 cannot be separated by means of any (HR-)IRMS instrumentation (Table 1), all approaches to determine $\Delta^{17}\text{O}$ in CO_2 base on elaborate chemical conversion and/or isotope exchange. Although the Ultra does not allow the separation of bulk CO_2 isotopologues, it does (in contrast to classical low resolution IRMS) allow the separation of the atomic fragments $^{17}\text{O}^+$, $^{18}\text{O}^+$, and $^{13}\text{C}^+$ ions from their typical water (^{16}OH , H_2^{16}O) and methylene (CH) interferences. This opens up a novel straight-forward approach to directly determine $\delta^{17}\text{O}$, $\delta^{18}\text{O}$, and $\delta^{13}\text{C}$ from CO_2 with high precision.

Instrumentation

The Ultra HR-IRMS (Figure 1 and 2) is a double-focusing gas source isotope ratio mass spectrometer with a flexible multicollector. The system employs Faraday cups and ion counters and is optimized, both in detector sensitivity and analyzer abundance sensitivity, for the detection of rare isotope species that are afflicted with isobaric interferences. Mass resolving powers $M/\Delta M > 30,000$ in high resolution mode ("flank steepness", 5%, 95% edge definition; reaching up to 50,000 for some applications) enable the full separation of isobaric interferences arising from ionization adducts, contaminants, fragments, and

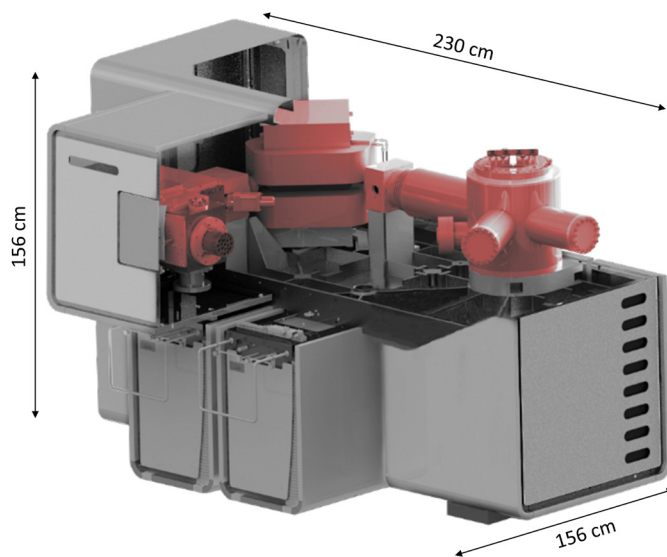


Figure 1. Interior schematics of the Ultra HR-IRMS. All hardware components relevant to the guiding of the ion beam path (shaded red) are mounted on a monolithic platform with a small footprint, for maximum ion optical stability. Electronic hardware (high voltage electronics, magnet, amplifier housing) is fully temperature-controlled, for maximum stability.

isotopologues of the analyte. To maximize transmission (i.e. ion yield), the instrument can be run in medium resolution mode, resulting in partially resolved isobaric interferences, where the analytes of interest can be directly measured on peak shoulders (Figures 3).

Conventional IRMS approaches to analyse $\delta^{13}\text{C}$ and $\delta^{18}\text{O}$ of CO_2

The $\delta^{13}\text{C}$ and $\delta^{18}\text{O}$ of CO_2 are traditionally deduced from the $^{13}\text{CO}_2/\text{CO}_2$ (mass ratio: 45/44) and $\text{CO}^{18}\text{O}/\text{CO}_2$ (mass ratio: 46/44) bulk isotope ratios. This approach requires systematic corrections (e.g. Assonov and Brenninkmeijer, 2003; Brand et al., 2010) to account for the unresolvable isobaric interferences of the ^{17}O -bearing CO_2 isotopologues (Table 1). Resolving these interferences calls for mass resolving powers between 11000 and 56000, whereas conventional IRMS instruments, such as the Thermo Scientific™ 253 Plus™, achieve ~1000.

Conventional IRMS approaches to analyse $\delta^{17}\text{O}$ of CO_2

The $\delta^{17}\text{O}$ cannot be inferred from CO_2 bulk isotope ratios because the ^{17}O -bearing isotopologues of CO_2 cannot be separated by means of IRMS instrumentation (Table 1). Consequently, a variety of sophisticated methods have been developed by the scientific community. All these methods rely on the indirect determination of the $\delta^{17}\text{O}$, based on elaborate chemical conversion and/or equilibration protocols. As a result, these methods are time-

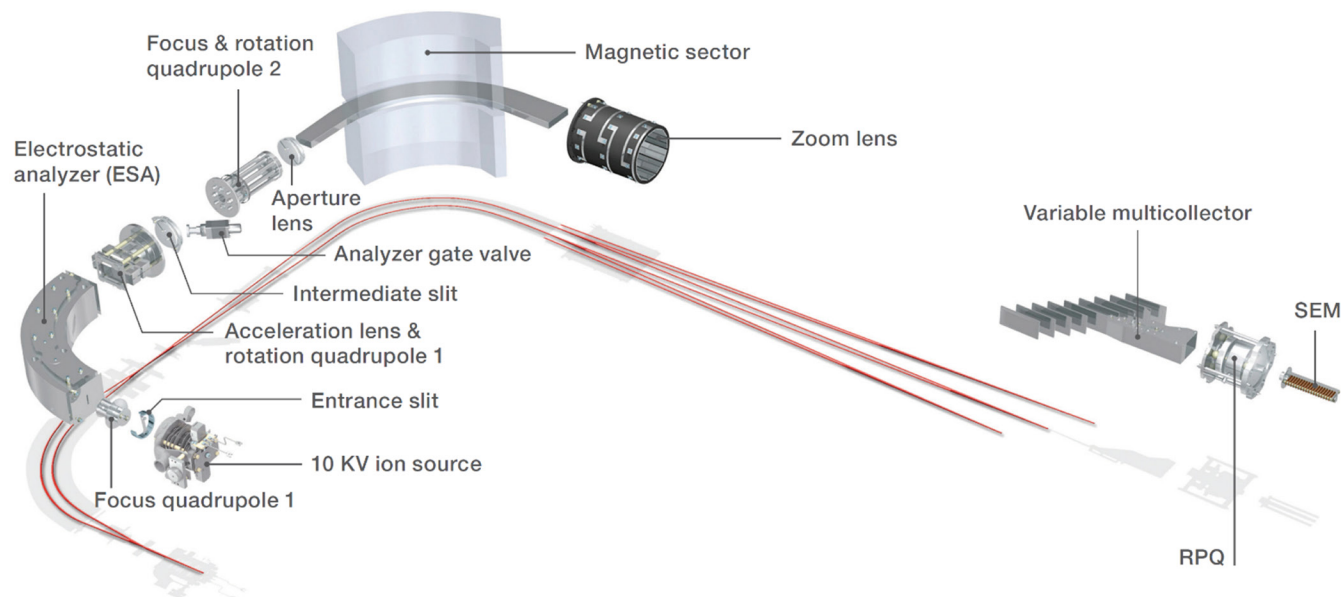


Figure 2: Ultra HR-IRMS ion beam path. The electrostatic analyzer is followed by the magnetic sector in the double-focusing Nier-Johnson type mass analyzer. Ions are accelerated to full potential before reaching the intermediate slit. Three sets of electromagnetic lenses prior to the electrostatic and magnetic sectors control the focusing of the ion beam, a zoom lens enables adjustment of dispersion. Signals are detected in an automated, variable position multicollector equipped with 9 dual channel collectors (8 of which are moveable) which comprise each a Faraday cup and an optional ion counter.

consuming and prone to the introduction of procedural errors during sample preparation and data processing:

1. Fluorination of CO_2 and isotopic analysis of the produced O_2 (Bhattacharya and Thiemens, 1989).
2. Conversion of CO_2 to H_2O and CH_4 followed by H_2O fluorination and isotopic measurement of the released O_2 (Brenninkmeijer and Röckmann, 1998)
3. Isotope exchange between CO_2 and CeO_2 with known oxygen isotopic composition and measurement of the $\delta^{45}\text{CO}_2$ value before and after exchange to calculate the $\delta^{17}\text{O}$ value of CO_2 (Assonov and Brenninkmeijer, 2001; Mahata et al., 2012; Mrozek et al., 2016)
4. Isotope exchange between CO_2 and CeO_2 followed by isotope analysis of the equilibrated CeO_2 by laser fluorination (Hofmann and Pack, 2010)
5. Equilibrium exchange of CO_2 with H_2O followed by fluorination of H_2O and measurement of the isotopic composition of released O_2 (Barkan and Luz, 2012; Passey et al., 2014)
6. Isotope exchange between CO_2 and O_2 over hot platinum and measurement of the isotopic composition of O_2 before and after exchange to calculate the $\delta^{17}\text{O}$ value of CO_2 (Mahata et al., 2013; Barkan et al., 2015; Adnew et al., 2019)

The HR-IRMS fragment approach to analyse $\delta^{13}\text{C}$, $\delta^{18}\text{O}$, and $\delta^{17}\text{O}$ of CO_2

The fragment approach makes use of the fragmentation of the sample CO_2 gas within the ion source. Next to CO_2^+ ions, fragment ions such as $^{12}\text{C}^+$, $^{13}\text{C}^+$, $^{16}\text{O}^+$, $^{17}\text{O}^+$, and $^{18}\text{O}^+$ are produced during ionization. Other than the analyses of bulk CO_2 ions, which cannot be separated by means of IRMS, the fragments can be readily analysed with HR-IRMS (Table 1) to directly measure, relative to a house standard, the carbon and triple oxygen isotopic composition (Adnew et al., 2019).

The fragment method requires the high-resolution capabilities of the Ultra HR-IRMS. In contrast to conventional IRMS, the Ultra's mass resolving power of up to $M/\Delta M > 30,000$ ("flank steepness", 5%, 95% edge definition) enables peak separation of $^{17}\text{O}^+$ and $^{18}\text{O}^+$ ions from their typical contaminants OH^+ and H_2O^+ , as well as the separation of the $^{13}\text{C}^+$ ion from the ionization adduct CH^+ .

HR-IRMS mass scans in Figure 3 and 4 illustrate partial peak separation for the carbon and oxygen fragments, demonstrating that the $^{13}\text{C}^+$, $^{17}\text{O}^+$ and $^{18}\text{O}^+$ signals can be analysed free of interferences on the respective peak shoulder plateaus. The scans were obtained in medium resolution mode at mass resolving powers of

Table 1. Isotopologues of carbon and oxygen fragments and CO₂, listed with typical interferences. Typically achieved mass resolving power (MRP) of classical IRMS instruments such as the 253 Plus is ~1000, whereas the Ultra HR-IRMS routinely achieves MRP >30,000. Major isotopologue species bold. *MRP = Mass Resolving Power = M/ΔM (5%, 95% edge definition), calculated versus major isotopologue species.

Cardinal mass	Ion species	Type	[amu]	MRP*	Resolvable with IRMS?	Resolvable with HR-IRMS?
12	¹² C ⁺	isotopologue	12.0000		no interfering masses	
13	¹³ C ⁺	isotopologue	13.0034			
	¹² CH ⁺	adduct	13.0078		x	✓
16	¹⁶ O ⁺	isotopologue	15.9949	2909	no interfering masses	
17	¹⁷ O ⁺	isotopologue	16.9991			
	¹⁶ OH ⁺	contaminant	17.0027	4712	x	✓
	¹³ CH ₄ ⁺	isotopologue	17.0347			
18	¹² CH ₅ ⁺	adduct	17.0391	3811	x	✓
	¹⁸ O ⁺	isotopologue	17.9992			
18	¹⁶ OH ₂ ⁺	contaminant	18.0106	1578	x	✓
	¹² C ¹⁶ O ₂ ⁺	isotopologue	43.9898		no interfering masses	
45	¹³ C ¹⁶ O ₂ ⁺	isotopologue	44.9932			
	¹² C ¹⁷ O ¹⁶ O ⁺	isotopologue	44.9940	52178	x	x
	¹⁴ N ¹⁵ N ¹⁶ O ⁺	contaminant	44.9981	9157	x	✓
46	¹² C ¹⁸ O ¹⁶ O ⁺	isotopologue	45.9941			
	¹³ C ¹⁷ O ¹⁶ O ⁺	isotopologue	45.9974	13983	x	✓
	¹² C ¹⁷ O ¹⁷ O ⁺	isotopologue	45.9983	11218	x	✓
	¹⁴ N ¹⁴ N ¹⁸ O ⁺	contaminant	46.0053	4094	x	✓
47	¹³ C ¹⁸ O ¹⁶ O ⁺	isotopologue	46.9974			
	¹² C ¹⁷ O ¹⁸ O ⁺	isotopologue	46.9983	54502	x	x
	¹³ C ¹⁷ O ¹⁷ O ⁺	isotopologue	47.0016	11218	x	✓
	¹⁵ N ¹⁵ N ¹⁶ O ⁺	contaminant	47.0023	9565	x	✓
	¹⁵ N ¹⁶ O ¹⁶ O ⁺	contaminant	46.9899	6274	x	✓
	¹² C ³⁵ Cl ⁺	contaminant	46.9689	1645	x	✓
48	¹² C ¹⁸ O ¹⁸ O ⁺	isotopologue	47.9983			
	¹³ C ¹⁷ O ¹⁸ O ⁺	isotopologue	48.0016	14427	x	✓
	¹⁴ N ¹⁸ O ¹⁶ O ⁺	contaminant	47.9971	40990	x	✓
	³² S ¹⁶ O ⁺	contaminant	47.9670	1532	x	✓
	¹³ C ³⁵ Cl ⁺	contaminant	47.9722	1838	x	✓
49	¹³ C ¹⁸ O ¹⁸ O ⁺	isotopologue	49.0017			
	¹⁵ N ¹⁸ O ¹⁶ O ⁺	contaminant	48.9942	6541	x	✓
	³³ S ¹⁶ O ⁺	contaminant	48.9664	1388	x	✓
	¹² C ³⁷ Cl ⁺	contaminant	48.9659	1370	x	✓
	C ⁴ H	contaminant	49.0078	7966	x	✓

~14,000 (accelerating voltage: 10 kV, source slit width: 16 μm, collector slit width: 800 μm or 1300 μm). Full peak separation in high resolution mode is omitted in favor of higher transmission. For the detection of the less abundant ¹³C⁺ and ¹⁷O⁺ species the Thermo Scientific™ 10¹³ Ω Amplifier Technology™ (Thermo Scientific Smart Note SN30439, 2017) is employed.

As demonstrated by Adnew et al. (2019) the triple oxygen (δ¹⁷O and δ¹⁸O) and carbon (δ¹³C) isotopic compositions of CO₂ can be directly (i.e. free of interferences) determined with high precision (Table 2) using the Ultra HR-IRMS by analysing the atomic fragments of C and O. Long measurement times in classical Dual Inlet mode can be reduced by applying the principle of Long Integration Dual Inlet (LIDI) mode. LIDI mode employs one extended

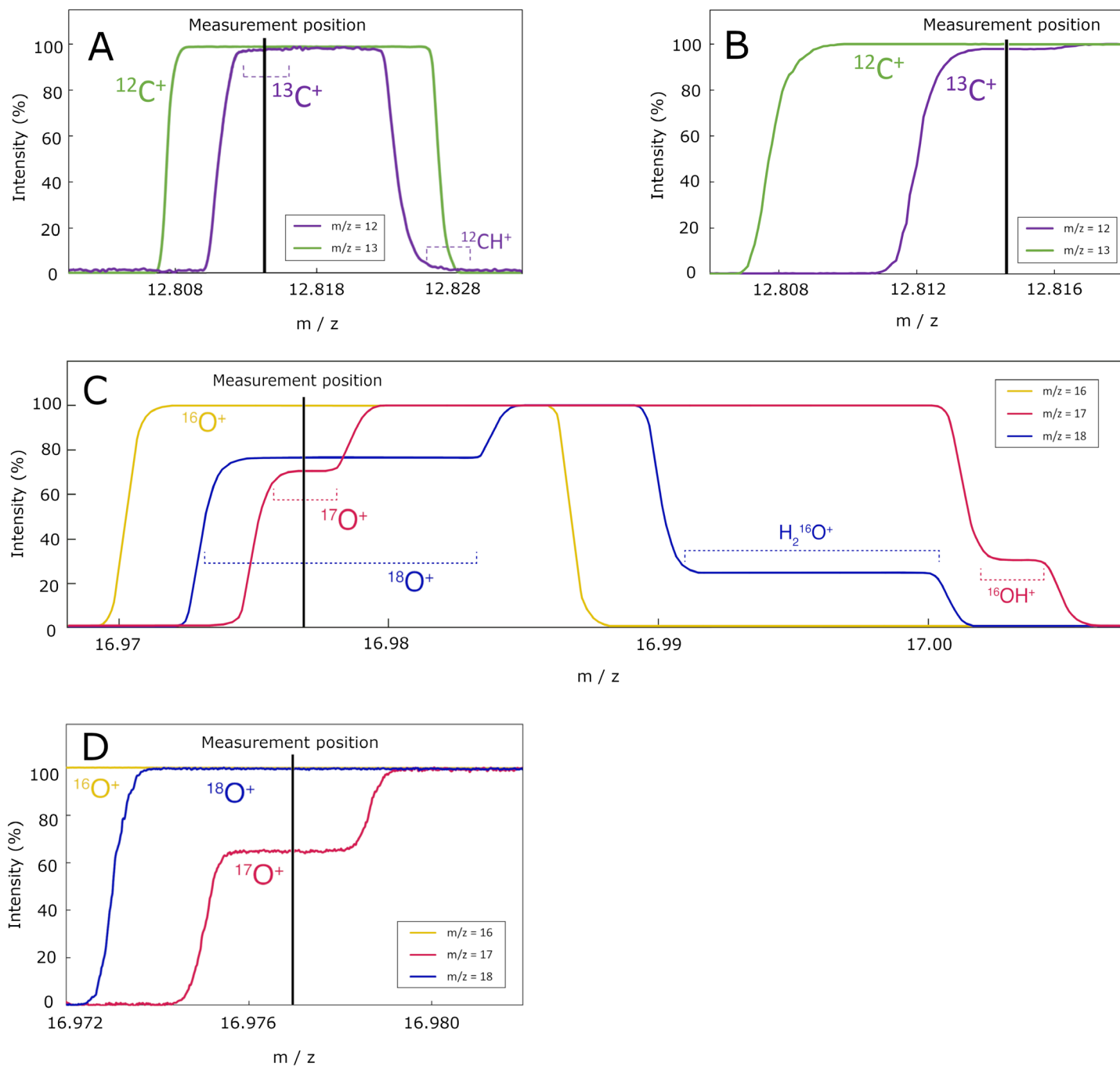


Figure 3. (A) Mass scan across the interference-free peak plateau of $^{13}\text{C}^+$ in medium resolution with $\text{MRP} \sim 14,000$. The $^{13}\text{C}^+$ ions are partially resolved from their methylene interference ($^{12}\text{CH}^+$). The $^{13}\text{C}^+$ peak shoulder plateau is aligned with $^{12}\text{C}^+$ for simultaneous analysis, measurement position is indicated by black vertical line. The $^{13}\text{C}^+$ signal is detected with a $10^{13} \Omega$ amplifier at a signal intensity of approximately 3,000,000 cps. **(B) Mass scan across a smaller scan range** emphasizes the flat $^{13}\text{C}^+$ plateau width of about 0.0025 m/z . Instrument mass stability is specified to <10 ppm, which translates to $<0.0002 m/z$. **(C) Mass scan across the interference-free peak plateaus of $^{16}\text{O}^+$, $^{17}\text{O}^+$, and $^{18}\text{O}^+$ in medium resolution with $\text{MRP} \sim 14,000$.** The $^{17}\text{O}^+$ and $^{18}\text{O}^+$ ions are partially resolved from their water interferences (^{16}OH and H_2^{16}O). The peak shoulder plateaus of all three oxygen species are aligned for simultaneous analysis, measurement position is indicated by black vertical line. The ^{17}O signal is detected with $10^{13} \Omega$ Amplifier Technology at a signal intensity of approximately 500,000 cps. **(D) Mass scan across a smaller scan range** emphasizes the flat $^{17}\text{O}^+$ plateau width of about 0.0025 m/z . Instrument mass stability is specified to <10 ppm, which translates to $<0.0002 m/z$.

sample gas acquisition which is compared to one extended reference gas acquisition, saving up to 50% sample gas and effective measurement time by dispensing changeover switching and related equilibration times (Müller et al., 2017; Thermo Fisher Smart Note SN30672; Thermo Scientific Technical Note TN30668).

How does the fragment approach push paleoclimate research forward?

Conventional isotope ratio mass spectrometry (IRMS) is routinely applied throughout the scientific community. The commonly analysed carbon and oxygen isotope signatures ($\delta^{13}\text{C}$ and $\delta^{18}\text{O}$) of CO_2 released from carbonates are essential tools to tackle the demanding scientific questions in paleoclimate research. However, these tools reach their limits when it comes to the identification of ancient carbonate formation mechanisms and to absolute geothermometry (for a general overview the reader is referred to Kasting et al., 2006).

The triple oxygen isotopes ($\delta^{18}\text{O}$ and $\Delta^{17}\text{O}$) reach beyond these limitations and offer an additional isotopic dimension which aids in deciphering past climate conditions. Tiniest variations in $\Delta^{17}\text{O}$ record fluid-rock interaction and diagenetic effects, not only in carbonates but also in silicates, sulfates, water, and air (e.g. Sharp and Wostbrock, 2021; Wostbrock et al., 2020; Sengupta et al., 2020;

Jäger et al., 2020). When combined with $\delta^{18}\text{O}$, the $\Delta^{17}\text{O}$ of carbonate CO_2 has potential to provide a single-phase carbonate geothermometer which requires no assumptions to be made about isotopic compositions of the ancient seawater the carbonate precipitated from (Surma et al., 2019). Figure 4 illustrates the concept of $\Delta^{17}\text{O}$ -thermometry in carbonates and the potential of combined $\delta^{18}\text{O}$ and $\Delta^{17}\text{O}$ to decipher diagenetic processes. Calcite samples that formed in equilibrium with seawater at a given temperature can be identified as they plot on the equilibrium curve in Figure 4. Their position along the curve reflects their formation temperature. Samples which plot apart from the equilibrium curves can constrain the degree of diagenesis and the isotopic composition of the diagenetic fluid. The arrows in Figure 4 represent exemplary trends of diagenetic effects, which can be modelled based on the initial (unaltered) equilibrium isotopic composition of the carbonate, the fluid/rock ratio, and the isotopic composition of the diagenetic fluid.

The fragment approach is a straightforward and independent alternative to conventional triple oxygen isotope analysis of carbonates. It deprives the need for sophisticated sample preparation and data processing to correct for interfering masses.

Table 2. Overview of typical accuracy and precision as achieved in different Ultra HR-IRMS laboratories (Utrecht University, IMAU, Utrecht; University of Göttingen, GZG, Göttingen) for total measurement durations of 3-12 hours. Values in brackets from long-term measurement of 24 hours. Note that sample consumption for LIDI analyses is reduced by about 50%.

		Dual Inlet		LIDI
		IMAU (Adnew et al., 2019)	GZG (Adnew et al., 2019)	GZG (unpublished)
Internal precision 1 s.e. [ppm]	$\delta^{13}\text{C}$	15	15	n.d.
	$\delta^{17}\text{O}$	37 – 82	21 – 35 (14)	20
	$\delta^{18}\text{O}$	11 – 25	7 – 17 (5)	8
External reproducibility 1 s.d. [ppm]	$\delta^{13}\text{C}$	15	20	n.d.
	$\delta^{17}\text{O}$	19	16	15
	$\delta^{18}\text{O}$	21	20	20

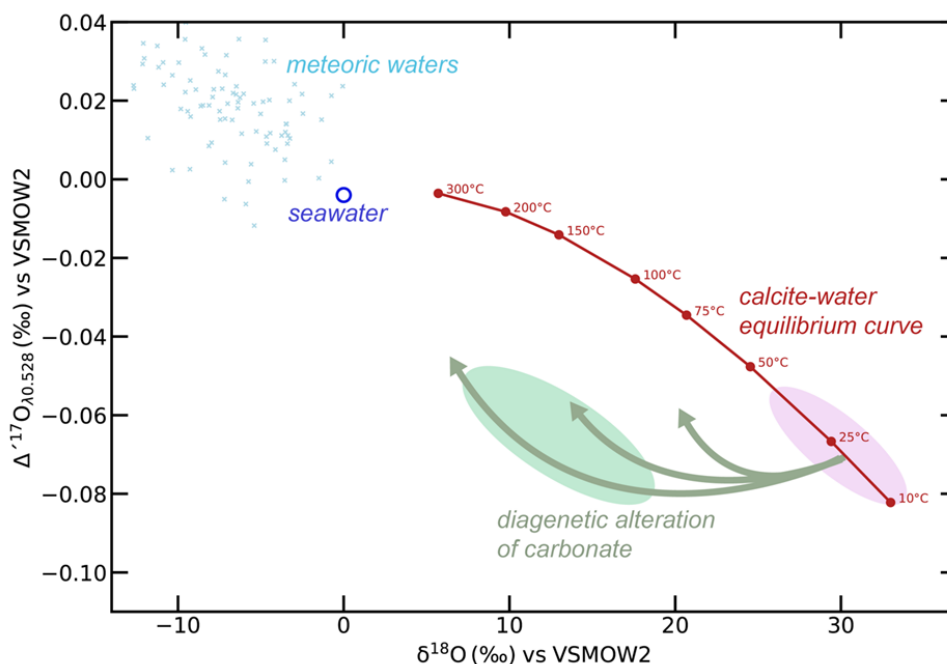


Figure 4: Conceptual illustration of $\Delta^{17}\text{O}$ -thermometry of carbonates and applicability of $\Delta^{17}\text{O}$ to decipher diagenetic processes in the carbonate-water system in the triple oxygen isotope space. The isotopic composition of calcite which precipitates in equilibrium with seawater (open blue circle, Luz & Barkan, 2010) is defined by the calcite equilibrium curve (red line, Wostbrock et al., 2020). Lower formation temperature results in higher $\delta^{18}\text{O}$ and lower $\Delta^{17}\text{O}$ of the calcite, whereas higher temperature results in lower $\delta^{18}\text{O}$ and elevated $\Delta^{17}\text{O}$. The red shaded field illustrates where carbonates that formed in equilibrium with seawater at 10–40 °C would plot. Carbonates that fall below the equilibrium curve may either suggest i) diagenetic (secondary) alteration of pristine carbonates by re-equilibration with seawater or meteoric waters (light blue crosses, Luz and Barkan, 2010), or ii) kinetic isotope effects during calcite formation (Guo and Zhou, 2019). The green shaded field schematically illustrates where calcite that was diagenetically altered by seawater or meteoric waters would plot.

Besides the triple oxygen isotopes of CO_2 , the field of clumped carbonate isotopes has recently experienced a strong upswing (e.g. Fiebig et al., 2019; 2021; Bajnai et al., 2020). Dual clumped carbonate analyses (Δ_{47} and Δ_{48}) of sedimentary carbonates allow for the quantitative determination of carbonate formation temperatures devoid of kinetic biases which may arise from incomplete isotopic equilibrium during mineral precipitation. This approach promises to significantly refine our ability to reconstruct and understand past climates. Clumped carbonate analyses are traditionally performed on low-resolution IRMS instrumentation, such as the Thermo Scientific™ 253 Plus™ and require comprehensive data processing to theoretically correct for unresolvable CO_2 isotopologue interferences on masses 47 and 48 (Table 1).

The fragment approach has potential to significantly contribute to the reliability of clumped carbonate data: The parallel determination of both the clumped signatures (Δ_{47} and Δ_{48}), and triple oxygen isotopes ($\delta^{17}\text{O}$ and $\delta^{18}\text{O}$) in a given CO_2 sample enables a direct and practical interference correction to clumped isotope measurements.

Besides the fragment approach, a general advantage of HR-IRMS for clumped carbonate data becomes apparent from Table 1. HR-IRMS can routinely resolve all contaminant-induced isobaric interferences on CO_2 . These interferences remain hidden for classical IRMS and may potentially introduce systematic biases in clumped carbonate data.

Summary of the benefits of the fragment approach and HR-IRMS in paleoclimate research

- **Alternative and robust method:** Isotope ratio measurements of atomic fragment ions ($^{12}\text{C}^+$, $^{13}\text{C}^+$, and $^{16}\text{O}^+$, $^{17}\text{O}^+$, $^{18}\text{O}^+$) of CO_2 provide an independent and robust alternative to determine the carbon ($\delta^{13}\text{C}$) and triple oxygen ($\Delta^{17}\text{O}$, $\delta^{18}\text{O}$) isotopic composition of carbon dioxide without the need for chemical processing or correction protocols for interfering masses.
- **Applicability to other gases:** The fragment approach can analogously be applied to other gases (N_2O , CO , CH_4 , C_2H_6 , C_3H_8 , ...) as well. As an example, $^{13}\text{C}^+$ in CH_4 could be directly analysed because it is readily

resolvable from $^{12}\text{C}^+$ by HR-IRMS. This circumvents the need for correction of the CH_5 adduct on $^{13}\text{CH}_4$, which is unresolvable by conventional IRMS. In larger hydrocarbons it can be applied to determine site-specific $\delta^{13}\text{C}$ compositions. In N_2O it can be used to analyse the site-specific distribution of ^{15}N . Note that comprehensive HR-IRMS applications have evolved already for methane (Thermo Scientific White Paper WP30767), larger hydrocarbons (Piasecki et al., 2018; Clog et al., 2018), and nitrous oxide (Magyar et al., 2016).

- **Advancing clumped carbonate analysis:** Clumped carbonate (Δ_{47} and Δ_{48}) measurements can benefit from accompanying fragment analyses. The $\delta^{17}\text{O}$, $\delta^{18}\text{O}$, and $\delta^{13}\text{C}$, as directly determined from CO_2 by HR-IRMS, can be utilized as a framework for absolute isotopologue interference corrections of the clumped signatures to improve reliability of clumped carbonate data.
- **A single-phase thermometer:** Combined analysis of $\delta^{17}\text{O}$ and $\delta^{18}\text{O}$ provides a high-precision tool for single phase paleothermometry (Surma et al., 2019; Jäger et al., 2020), and a proxy to identify the preservation of pristine carbonate. It is possible to distinguish whether triple oxygen isotopes reflect equilibrium formation conditions (i.e. no alteration), or a diagenetic overprint after deposition.

References

1. Adnew, G.A., Hofmann, M.E.G., Paul, D., Laskar, A., Surma, A., Albrecht, N., Pack, A., Schwieters, J., Koren, G., Peters, W., and Röckmann, T. (2019) Determination of the triple oxygen and carbon isotopic composition of CO_2 from atomic ion fragments formed in the ion source of the 253 Ultra High-Resolution Isotope Ratio Mass Spectrometer. *Rapid Commun Mass Spectrom*, 30(17), 1363-1380, doi:10.1002/rcm.8478
2. Adnew, G.A., Pons, T.L., Koren, G., Peters, W., and Röckmann, T. (2020) Leaf-scale quantification of the effect of photosynthetic gas exchange on $\Delta^{17}\text{O}$ of atmospheric CO_2 . *Biogeosciences*, 17, 3903-3922.
3. Assonov, S.S., Brenninkmeijer, C.A. (2001) A new method to determine the ^{17}O isotopic abundance in CO_2 using oxygen isotope exchange with a solid oxide. *Rapid Commun Mass Spectrom*, 15(24), 2426-2437.
4. Assonov, S.S., and Brenninkmeijer, C.A. (2003) On the ^{17}O correction for CO_2 mass spectrometric isotopic analysis. *Rapid Commun Mass Spectrom*, 17(10), 1007-1016.
5. Bajnai, D., Guo, W., Spötl, C. et al. (2020) Dual clumped isotope thermometry resolves kinetic biases in carbonate formation temperatures. *Nat Commun* 11(4005).
6. Barkan, E. and Luz, B. (2012) High-precision measurements of $^{17}\text{O}/^{16}\text{O}$ and $^{18}\text{O}/^{16}\text{O}$ ratios in CO_2 . *Rapid Commun Mass Spectrom*, 26(23), 2733-2738.
7. Barkan, E., Musan, I., Luz, B. (2015) High-precision measurements of $\delta^{17}\text{O}$ and ^{17}O -excess of NBS19 and NBS18. *Rapid Commun Mass Spectrom*, 29(23), 2219-2224.
8. Bhattacharya, S.K., and Thiemens M.H. (1989). New Evidence for Symmetry Dependent Isotope Effects O+CO Reaction. *Zeitschrift für Naturforschung*, 44a, 435-444.
9. Brand, W.A., Assonov, S.S., and Coplen, T.B. (2010) Correction for the ^{17}O interference in $\delta^{13}\text{C}$ measurements when analyzing CO_2 with stable isotope mass spectrometry (IUPAC Technical Report). *Pure Appl Chem*, 82(8), 1719-1733, doi:10.1351/PAC-REP-09-01-05
10. Brenninkmeijer, C.A.M., Röckmann, T. (1998) A Rapid Method for the Preparation of O_2 from CO_2 for Mass Spectrometric Measurement of $^{17}\text{O}/^{16}\text{O}$ Ratios. *Rapid Commun Mass Spectrom*, 12, 479-483.
11. Clog, M., Lawson, M., Peterson, B., Ferreira, A. A., Neto, E. V. S., & Eiler, J. M. (2018). A reconnaissance study of ^{13}C - ^{13}C clumping in ethane from natural gas. *Geochim Cosmochim Acta*, 223, 229-244.
12. Farquhar, J., Thiemens, M.H., Jackson, T. (1998) Atmosphere-surface interactions on Mars: $\Delta^{17}\text{O}$ measurements of carbonate from ALH 84001. *Science*, 280(5369), 1580-1582.
13. Fiebig, J., Bajnai, D., Löffler, N., Methner, K., Krsnik, E., Mulch, A., Hofmann, S. (2019) Combined high-precision Δ_{48} and Δ_{47} analysis of carbonates. *Chem Geol*, 522, 186-191.
14. Fiebig, J., Daëron, M., Bernecker, M., Guo, W., Schneider, G., Boch, R., Bernasconi, S.M., Jautzy, J., Dietzel, M. (2021) Calibration of the dual clumped isotope thermometer for carbonates. *Geochim Cosmochim Acta*, (in press, <https://doi.org/10.1016/j.gca.2021.07.012>).
15. Guo, W., Zhou, C. (2019) Triple oxygen isotope fractionation in the DIC- H_2O - CO_2 system: A numerical framework and its implications. *Geochim Cosmochim Acta*, 246, 541-564.
16. Hoag, K.J., Still, C.J., Fung, I.Y., Boering, K.A. (2005) Triple oxygen isotope composition of tropospheric carbon dioxide as a tracer of terrestrial gross carbon fluxes. *Geophysical Research Letters*, 32(2)
17. Hofmann, M.E.G. and Pack, A. (2010) Technique for high-precision analysis of triple oxygen isotope ratios in carbon dioxide. *Anal Chem*, 82(11), 4357-4361.
18. Hofmann, M.E.G., Horváth, B., Schneider, L., Peters, W., Schuetzenmeister, K., Pack, A. (2017) Atmospheric measurements of $\Delta^{17}\text{O}$ in CO_2 in Göttingen, Germany reveal a seasonal cycle driven by biospheric uptake. *Geochim Cosmochim Acta*, 199, 143-163.
19. Jäger, O., Surma, J., Albrecht, N., Marien, C. S., Xiang, W., Schier, K., Bau, M., Reitner, J., Pack, A. (2020) High-precision triple oxygen isotope analysis of Archean and Proterozoic carbonates. EGU General Assembly, EGU2020-17881.

20. Kasting, J.F., Tazewell Howard, M., Wallmann, K., Veizer, J., Shields, G., Jaffrés, J. (2006) Paleoclimates, ocean depth, and the oxygen isotopic composition of seawater. *Earth Planet Sci Lett*, 252(1-2), 82-93
21. Koren, G., Schneider, L., van der Velde, I.R., van Schaik, E., Gromov, S.S., Adnew, G.A., (2019). Global 3-D simulations of the triple oxygen isotope signature $\Delta^{17}\text{O}$ in atmospheric CO_2 . *JGR Atmospheres*, 124
22. Liang, M.C., Blake, G.A., Lewis, B.R., Yung, Y.L. (2007) Oxygen isotopic composition of carbon dioxide in the middle atmosphere. *Proc Natl Acad Sci USA*, 104(1), 21-25.
23. Magyar, P. M., Orphan, V. J., & Eiler, J. M. (2016). Measurement of rare isotopologues of nitrous oxide by high-resolution multi-collector mass spectrometry. *Rapid Commun Mass Spectrom*, 30(17), 1923-1940.
24. Mahata, S., Bhattacharya, S.K., Wang, C.H., Liang, M.C. (2012) An improved CeO_2 method for high-precision measurements of $^{17}\text{O}/^{16}\text{O}$ ratios for atmospheric carbon dioxide. *Rapid Commun Mass Spectrom*, 26(17), 1909-1922.
25. Mahata, S., Bhattacharya, S.K., Wang, C.H., Liang, M.C. (2013) Oxygen isotope exchange between O_2 and CO_2 over hot platinum: an innovative technique for measuring $\Delta^{17}\text{O}$ in CO_2 . *Anal Chem*, 85(14), 6894-6901.
26. Miller, M.F. (2002) Isotopic fractionation and the quantification of ^{17}O anomalies in the oxygen three-isotope system: an appraisal and geochemical significance. *Geochim Cosmochim Acta*, 66(11), 1881-1889.
27. Mrozek, D.J., van der Veen, C., Hofmann, M.E.G., Chen, H., Kivi, R., Heikkinen, P., Röckmann, T. (2016) Stratospheric Air Sub-sampler (SAS) and its application to analysis of $\Delta^{17}\text{O}$ (CO_2) from small air samples collected with an AirCore. *Atmospheric Measurement Techniques*, 9(11), 5607-5620.
28. Müller, I.A., Fernandez, A., Radke, J., van Dijk, J, Bowen, D., Schwieters, J., Bernasconi, S.M. (2017) Carbonate clumped isotope analyses with the long-integration dual-inlet (LIDI) workflow: scratching at the lower sample weight boundaries. *Rapid Commun Mass Spectrom*, 31(12), 1057-1066.
29. Passey, B.H., Hu, H., Ji, H., Montanari, S., Li, S., Henkes, G.A., Levin, N.E. (2014) Triple oxygen isotopes in biogenic and sedimentary carbonates. *Geochim Cosmochim Acta*, 141, 1-25.
30. Sengupta, S., Peters, S.T.M., Reitner, J., Duda, J.P., Pack, A. (2020) Triple oxygen isotopes of cherts through time. *Chem Geol*, 554, 119789.
31. Thermo Scientific SmartNote SN30439 (2017) $10^{13} \Omega$ amplifier technology: How low can you go?
32. Piasecki, A., Sessions, A., Lawson, M., Ferreira, A. A., Neto, E. S., Ellis, G. S., & Eiler, J. M. (2018). Position-specific ^{13}C distributions within propane from experiments and natural gas samples. *Geochim Cosmochim Acta*, 220, 110-124.
33. Sharp, Z.D., Wostbrock, J.A.G. (2021) Standardization for the Triple Oxygen Isotope System: Waters, Silicates, Carbonates, Air, and Sulfates. *Rev Mineral Geochem*, 86, 179-196.
34. Surma, J., Albrecht, N., Jäger, O., Marien, C.S., Xiang, W., Reitner, J., Pack, A. (2019) Triple Oxygen Isotope Analysis in Carbonates – New Insights from High Resolution Mass Spectrometry. *Goldschmidt Abstracts*, 3275.
35. Thermo Fisher Smartnote SN30672 (2019) How do I measure clumped Δ_{47} from carbonates using the Thermo Scientific portfolio?
36. Thermo Scientific Technical Note TN30668 (2019) How do I measure clumped Δ_{47} from carbonates using the Thermo Scientific portfolio?
37. Thermo Scientific WhitePaper WP30767 (2021) Clumped isotope analysis of methane using HR-IRMS: New insights into origin and formation mechanisms of natural gases and a potential geothermometer.
38. Thiemens, M.H., Jackson, T., Zipf, E.C., Erdman, P.W., van Egmond, C. (1995) Carbon Dioxide and Oxygen Isotope Anomalies in the Mesosphere and Stratosphere. *Science*, 270 (5238), 969-972.
39. Thiemens, M.H. (1999) Mass-independent isotope effects in planetary atmospheres and the early solar system. *Science*, 283(5400), 341-345.
40. Thiemens, M.H., Chakraborty, S., Jackson, T.L. (2014) Decadal $\Delta^{17}\text{O}$ record of tropospheric CO_2 : Verification of a stratospheric component in the troposphere. *JGR Atmospheres*, 119(10), 6221-6229.
41. Wiegel, A.A., Cole, A.S., Hoag, K.J., Atlas, E.L., Schauffler, S.M., Boering, K.A. (2013) Unexpected variations in the triple oxygen isotope composition of stratospheric carbon dioxide. *Proc Natl Acad Sci USA*, 110(44), 17680-17685.
42. Wostbrock, J.A.G., Brand, U., Coplen, T.B., Swart, P.K., Carlson, S.J., Brearley, A.J., Sharp, Z.D. (2020) Calibration of carbonate-water triple oxygen isotope fractionation: Seeing through diagenesis in ancient carbonates. *Geochim Cosmochim Acta*, 288, 369-388.

Find out more at thermofisher.com/neoma

For Research Use Only. Not for use in diagnostic procedures. © 2021 Thermo Fisher Scientific Inc. All rights reserved. All trademarks are the property of Thermo Fisher Scientific Inc. and its subsidiaries unless otherwise specified. Elemental Scientific Lasers and NWR are trademarks of Elemental Scientific Inc. NIST and SRM are registered trademarks of the National Institute of Science and Technology. This information is presented as an example of the capabilities of Thermo Fisher Scientific Inc. products. For instrument specifications, please consult your local sales representative. It is not intended to encourage use of these products in any manners that might infringe the intellectual property rights of others. Specifications, terms and pricing are subject to change. Not all products are available in all countries. Please consult your local sales representative for details. **AN000231-EM-EN 1021S**